Enhanced Resonant Positron Annihilation due to Nonfundamental Modes in Molecules

S. Ghosh,* J. R. Danielson,† and C. M. Surko‡
Physics Department, University of California San Diego, La Jolla, California 92093, USA

(Received 4 July 2020; accepted 11 September 2020; published 23 October 2020)

Positrons attach to most molecules through Feshbach resonant excitation of fundamental vibrational modes, and this leads to greatly enhanced annihilation rates. In all but the smallest molecules, vibrational energy transfer further enhances these annihilation rates. Evidence is presented that in alkane and cycloalkane molecules, this can occur by the excitation of other than fundamental vibrations and produce roughly comparable annihilation rates. These features are compared to infrared absorption spectra. A possible mechanism is discussed that involves combination and overtone vibrations.

DOI: 10.1103/PhysRevLett.125.173401

Positron interactions with matter are important in a number of areas of science and technology, including atomic, plasma, and astrophysics, materials science, medicine, and biology [1–7]. While many phenomena are well studied, important questions remain. Here, evidence is reported of an enhanced resonant annihilation mechanism in positron interactions with molecules that does not involve fundamental vibrational modes. It is expected to be important in a number of physical situations.

The fate of a positron is considered when interacting with a molecule at energies below the threshold for electronic excitation and positronium formation. In addition to elastic and inelastic vibrational scattering, a positron at the resonant energy can excite a vibrational mode via a vibrational Feshbach resonance (VFR) and attach to the molecule. This results in increased probability of annihilation on a molecular electron [8].

The simplest such process is one in which the positron at the resonant energy E_r excites a dipole-allowed fundamental vibration with frequency ω_ν to become attached to the molecule, where

$$E_r = \hbar\omega_\nu - E_b, \tag{1}$$

where E_b is the positron-molecule binding energy. In this case, the annihilation rate is well described by a competition between annihilation on the molecule and the ejection of the positron by vibrational deexcitation [9]. However, if the fundamental couples to combination and overtone modes [i.e., by intramolecular vibrational energy redistribution (IVR)], the fate of the positron depends upon the coupling of the daughter modes to the positron continuum; the positron may escape more quickly (an "escape channel") or remain on the molecule longer (a "dark state"), with the former leading to a smaller, and the later leading to a larger annihilation rate [8]. While IVR-enhanced VFR are frequently observed and possible models have been discussed [8,10,11], a detailed theory of this process has yet to be formulated. These resonances ride on a broad background of annihilation which is also above the level expected from a simple collision process. There is indirect evidence that this background is due to annihilation on combination and overtone vibrations [8,11,12].

In this Letter, we present evidence for the existence of another type of enhanced resonant annihilation process. Annihilation spectra as a function of incident positron energy are studied for cycloalkane, C_nH_{2n}, and alkane molecules, C_nH_{2n+2} for $5 \le n \le 8$. New features are observed in the region close to, but below, the C-H stretch vibrational modes. These resonances have enhanced annihilation rates as large as 30% of the peak rates of the IVR-enhanced C-H stretch resonances. The energies of these resonances are compared with infrared (IR) absorption spectra which is a monitor of dipole-allowed transitions. The correspondence between the two sets of spectra is discussed.

The most straightforward explanation is that these new features are due to multimode vibrations. If so, they could be of considerable importance. For example, they would be dominant when the binding energy of the molecule is larger than the highest-energy fundamental vibration [i.e., then $E_r < 0$ in Eq. (1)]. This occurs in the heavy halomethanes such as CBr_4 [13]. Another example is the larger polycyclic aromatic molecules, such as pyrene, which are relevant for positron annihilation in the interstellar medium [14,15].

The experimental apparatus and procedures have been described in detail elsewhere [8,16,17]. Positrons from a ^{22}Na radioactive source are moderated to electron-volt energies using a layer of solid Ne at 8 K [18,19] then magnetically guided into a Penning-Malmberg-style buffer gas trap (BGT) at 293 K. They thermalize to the ambient via inelastic collisions with N_2 and CF_4 molecules. The cold positrons are then extracted in a magnetically guided, pulsed beam at a 2 Hz rate (the BGT beam). One molecule [cyclopentane (C_5H_{10})] was also studied using a cryogenically cooled positron beam (CT beam) generated in a separate trap through collisions with CO molecules at 50 K [17].

Application of a negative potential on the BGT confinement well was used to produce a slower mean beam energy (0.65 eV) than that used previously. This permits improved control of the number of transits through the test-gas cell. By adjusting the voltage on the gas cell, the energy of the positron beam in the cell is tunable to as low as from 50 meV for the BGT beam and to 25 meV for CT beam. The other parameters of these exponentially modified Gaussian (EMG) [20] distributions are the positron temperature T, which determines motion in the plane perpendicular to the magnetic field and the width σ of the Gaussian parallel energy distribution. For the BGT and CT beams, respectively, T is 20 and 5 meV, and the σ values are 10 and 8 meV.

The test-gas pressure is maintained in range 3–30 μtorr. Total scattering is kept to $\lesssim 10\%$ to avoid multiple scattering. Annihilation is monitored using a CsI detector to record single annihilation γ-ray counts during the 14 μs time interval for positron to make one round trip through the cell. To minimize simultaneous annihilation events and miscounting, the count rate is kept $\lesssim 0.2$ per pulse by adjusting the pressure, number of positrons per pulse, and the detector position. In the absence of the target gas, the cell is used as a retarding potential analyzer to measure the parallel energy distribution of the positron beam [20].

The distributions $f(\hat{E}, E)$ in total energy E of the beams, where $\hat{E}$ is the peak of the distribution, are EMGs. They are obtained using $f(E)$ from Eq. (5) of Ref. [20], the measured parallel energy distribution, and $df(E)/dE = 0$ (which defines $\hat{E}$).

The number of positrons per pulse and transits through the gas cell, the test-gas pressure, and the path length as viewed by the detector are used to determine the normalized annihilation rate Z_{eff} [8,16]. Here, Z_{eff} is defined as the annihilation rate divided by that for a gas of free electrons with number density equal to the molecular density. Measurements of Z_{eff} were verified to have the expected dependence on gas pressure, positrons per pulse, and detector positron. The noise in the data is statistical and proportional to the square root of the number of detected γ rays. Systematic errors are estimated to be $< 15\%$.

Figure 1 shows the resonant annihilation amplitude Z_{eff} as a function of the peak energy of the beam $\hat{E}$ for cyclopentane, C_5H_{10}, using both the BGT and CT beams. The large peak at ~315 meV is approximately that expected for an IVR-enhanced VFR (which we denote as resonances R_1) due to the two dipole-allowed C-H stretch vibrations, one of which is degenerate [21–23]. However, extra spectral weight is observed on the low-energy side of the C-H peak [cf. Fig. 1(a) inset]. Making the hypothesis that this structure is due to one or more new resonances which are narrow in energy compared to the beam energy resolution, Figure 1(b) shows the resulting fit (corresponding IR spectrum in the inset), and Fig. 1(c) shows the decomposition into the individual resonances.

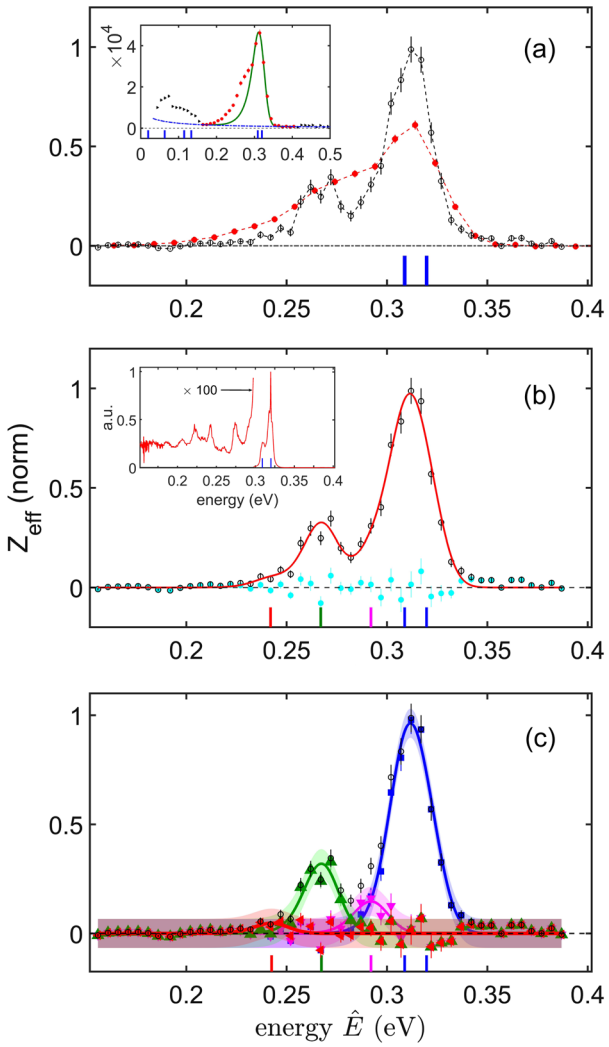

FIG. 1. The annihilation rate Z_{eff} for cyclopentane ($E_b = 48$ meV) as a function of peak total energy $\hat{E}$. (a) Background-subtracted Z_{eff} in the region near the C-H stretch peak for the CT (open circle) and BGT (red solid circle) beams. Data in (a), (b), and (c) are normalized to the CT beam peak Z_{eff}, and dashed lines in (a) are guides to the eye. Error bars are those due to counting statistics. Inset shows absolute Z_{eff} using the BGT beam on a wider energy scale; (blue vertical bar) fundamental modes; (black right triangle) data not used in the analysis; (green curve) beam convoluted with the two fundamental C-H mode VFRs at the downshifted locations 309 and 320 meV; (blue dot-dashed line) is the background annihilation [13,24]. (b) Fits to the background-subtracted cryobeam data using three additional VFRs (beyond the C-H stretch peaks) located at 292, 267, and 242 meV (magenta, green, red vertical bars); (cyan solid circle) are the residuals. Inset shows the IR spectrum downshifted by the binding energy of 48 meV. (c) The fits to the three new resonances (magenta curve, down magenta triangle), (green curve, up green triangle), and (red curve, left red triangle), and the two C-H peaks (blue curve, blue square). For the VFR model considered here, the resonance positions are expected to be downshifted from the mode energies by E_b. Shaded regions are color coded to match the VFR and indicate the 95% confidence level.

To begin the analysis, a broad background, assumed to be $\propto 1/\hat{E}$ based upon previous work [11,13] [cf. dot-dashed line, Fig. 1(a) inset] is subtracted. The $Z_{\rm eff}$ spectrum is then written as a sum of IVR-enhanced VFR resonances (i.e., with each resonance the beam convolved with a delta function in energy) [25]. This sum includes the resonances R_1 and a number of unknown new resonances with adjustable amplitudes A_j located at energies E_j. Assuming electric-dipole excitation with elastic rate large compared to the annihilation rate, the result is [25,26]

$$Z_{\rm eff}(\hat{E}) = \sum_j A_j f(\hat{E}, E_j), \tag{2}$$

where

$$A_j = \pi F \beta_j g_j \sqrt{\frac{E_b}{E_j}}. \tag{3}$$

Here, $F = 0.66$ a measure of electron-positron overlap, β_j is the IVR enhancement factor [26], and g_j is the multiplicity of the vibration for fundamental modes [25].

The number of C-H peaks in the molecules studied varies from 3 to 12, spread over an energy range from 10 to 15 meV. Their amplitudes are not known. To simplify the analysis, they are combined into two resonances located at the edges of their respective energy range in order to model the spectrum close to the peak. Their energies are kept fixed, and they are included in Eq. (2) with adjustable amplitudes, A_1 and A_1'.

To determine whether the predictions of Eq. (2) are consistent with the observations, an additional unknown resonance R_2 is added with adjustable amplitude A_2 and at an unknown energy E_2'. Then, E_2' is varied with the amplitudes A_1, A_1', and A_2 adjusted for best fit to the data (i.e., a minimum in the rms error). If R_2 is present, there will be a minimum in the rms error in the total fit. This process is repeated introducing possible additional VFR, keeping the energies of previously determined VFR fixed, and using all amplitudes and the energy of the possible additional resonance as adjustable parameters until no additional resonant features are found. The number of additional resonances found in this way, beyond the C-H stretch peaks, varies from one to three for the data presented here. The decomposition for cyclopentane is shown in Fig. 1(c).

To ensure that this serial method of finding resonances did not introduce a bias, another method was also used to find additional resonances beyond R_1. Extra resonances were introduced spaced ~15–20 meV apart and at arbitrary positions below R_1. Their amplitudes and positions and A_1 and A_1' were allowed to vary to determine the best fit. The resulting resonant amplitudes and positions were consistent with the previous procedure for several molecules.

Results are shown in Figs. 1–3 for cyclopentane, cyclooctane, and heptane and reported in Table I. The table includes upshifted resonance locations $\hbar\omega_j = E_j + E_b$ and the peak $Z_{\rm eff}$ for each molecule, the IVR enhancement factors β_j, and a normalized amplitude $\tilde{A}_j$, which is A_j of the new VFR relative to that for the sum of the two the C-H stretch peaks, with the background subtracted from both quantities. It was verified that the peak positions and amplitudes were insensitive to ±50% changes in assumed background in the analysis region.

Resonances similar in character to those shown, but smaller in amplitude, were observed for pentane and hexane ($\tilde{A}_j = 9\%$ and 8%, respectively). While showing evidence of new VFRs, the analysis failed to give completely consistent results for BGT-beam measurements for cyclopentane, cyclohexane, cycloheptane, and octane (due to weak resonances and/or two resonances being too closely spaced). In all molecules, there could be resonances at smaller amplitudes that are below our noise level (e.g., the 68% confidence level $\tilde{A}_j \leq 3\%$). Because of technical difficulties, CT data are only available for cyclopentane.

The overall conclusion is that the measurements are consistent with additional resonant features below the C-H stretch resonances for the alkane and cycloalkane molecules studied. Thus, this may well be a general phenomenon in these types of molecules. The fits to the data for

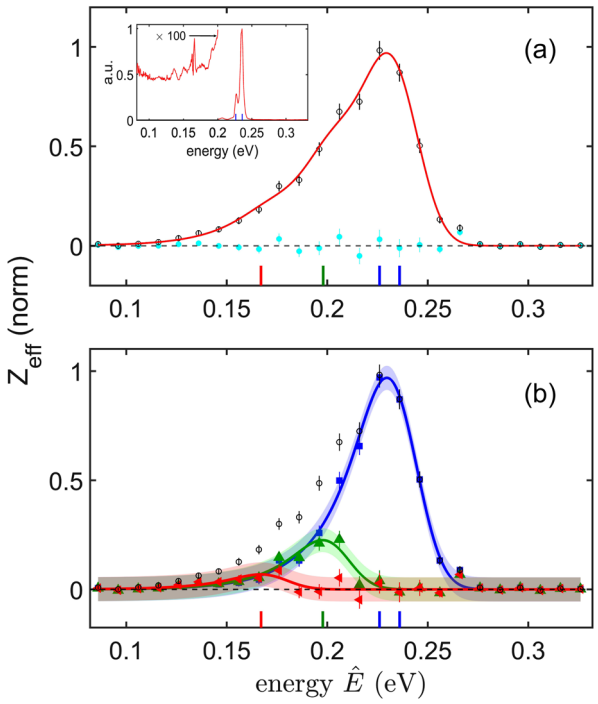

FIG. 2. Data and analysis for cyclooctane ($E_b = 128$ meV) using the BGT beam with the same procedures and notation as used in Figs. 1(b) and 1(c). Lower panel shows fits to the C-H peaks (blue curve, blue square) and two new resonances at 198 meV (green curve, green up triangle) and 167 meV (red curve, red left triangle).

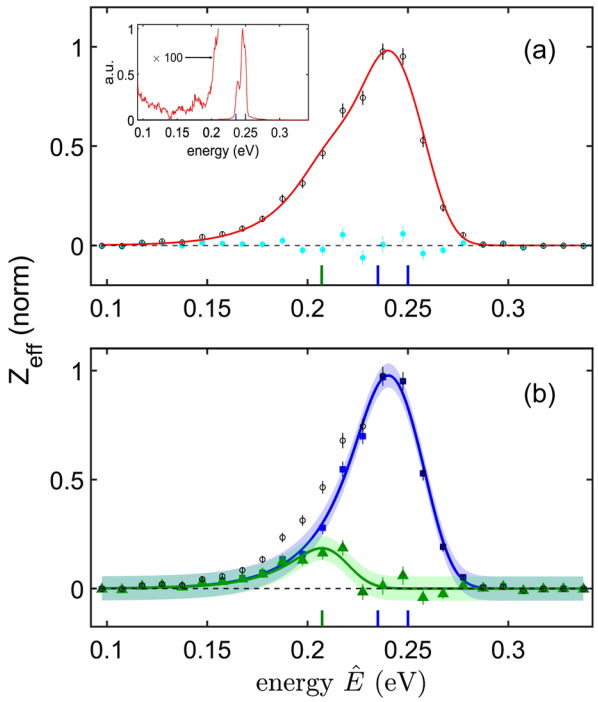

FIG. 3. Data and analysis for heptane ($E_b = 118$ meV) using the BGT beam with the same procedures and notation as used in Figs. 1(b) and 1(c). Lower panel shows fits to the C-H peaks (blue curve, blue square) and the one new resonance (green curve, green up triangle) at 207 meV.

the largest-amplitude VFR in each molecule listed in Table I indicate an uncertainty in the position of the peaks of approximately ±5 meV, in the widths (FWHM) of ±10 meV, and in A_j and β_j of ±16%. Thus, the new features are consistent with resolution-limited VFR similar to the C-H stretch resonances. However, features as broad as ∼10 meV FHWM (or multiple sharp resonances extending over that energy interval) cannot be ruled out.

The origin of these new resonances is presently unclear. Considering further the possibility that they are resolution-limited VFR, the simplest annihilation VFR are explained by assuming that the positron excites a dipole-allowed vibrational transition. This implies that there will be infrared (IR) absorption at the position of this vibrational mode. The existence of the new resonances led us to consider whether they may also be associated with IR activity [e.g., Figs. 1(b), 2(a), and 3(a) insets] [27]. The IR spectra exhibit peaks riding on a broad background. Table I gives the locations of the IR peaks, which are found to be within ±7 meV of the new VFR. However, many other IR peaks in the region of energies studied do not appear to be associated with new VFR activity. Thus, if there is such a correspondence between the IR spectrum and new VFR, there appears to be an additional constraint (a selection principle) on the occurrence of the new VFR that is presently unclear.

It is plausible that these new resonances are due to combination and/or overtone vibrations. Unfortunately, there are a relatively large number of combination vibrations in the molecules studied, even restricting candidates to two-mode combinations, and so it is hard to identify which particular modes might be responsible. A related question is, if multimode vibrations are responsible, why do only a small number (i.e., 1–3 extra VFR) dominate the additional spectral weight? Here again, if there is a "selection principle," what is it?

With regard to the dipole-allowed-excitation question and the possibility of IVR enhancement, we note that there are non-dipole-allowed modes for which the combination mode is dipole allowed. This would be an appealing explanation in that each of the constituent modes is a good candidate for a dark state (i.e., producing IVR enhancement), while excitation of the combination mode is a dipole-allowed transition (a "doorway state").

In summary, presented here is evidence of new IVR-enhanced VFR that are not due to fundamental vibrational modes. An analysis was presented that provides a reasonable fit to the data assuming a small number of new resonances broadened by the positron beam energy

TABLE I. VFR analyses for the two ring alkanes and a chain alkane: CT data for cyclopentane and BGT data for cyclooctane and heptane. Z_{eff} is the maximum value for each molecule and E_b the binding energy. The C-H modes are grouped into two resonances with positions $\hbar\omega_\nu$, effective mode degeneracy g_ν, and amplitude β_ν. New resonance locations are upshifted by E_b to $\hbar\omega_j = E_j + E_b$ to compare with IR spectra [27]; β_j are the new-IVR enhancement factors and $\tilde{A}_j$ the normalized amplitudes. All energies are in meV. See text for details.

Molecule	Z_{eff} $\times 10^{-3}$	E_b	$\hbar\omega_\nu$	g_ν	β_ν	$\hbar\omega_j$	β_j	$\tilde{A}_j$	Nearest IR peak
C_5H_{10}	74	48	357	2	27	340	10	14	339, 342
			368	1	32	315	22	31	308, 322
						290	3	5	290
C_8H_{16}	831	128	354	5	89	326	176	22	320
			364	3	136	295	52	7	294
C_7H_{16}	611	118	353	5	72	325	112	18	324, 331
			368	6	61				

distribution. It is hoped that this study will motivate theoretical work on IVR enhancement of combination and overtone vibrations as well as other possible origins of these new features. As mentioned above, the conclusion that these new resonant features are due to other than VFR due to fundamental vibrations has interesting physical implications. There is a class of molecules that have positron binding energies exceeding that of the highest-energy fundamental mode (e.g., larger polycyclic aromatic molecules). In this case, annihilation of low-energy positrons can be expected to be dominated by other than fundamental-mode resonances such as those described here.

We thank G. Gribakin for helpful conversations. This work was supported by the NSF, Grants No. PHY-1702230 and No. PHY-2010699.

*soumen@physics.ucsd.edu
†jrdanielson@ucsd.edu
‡csurko@ucsd.edu

[1] C. M. Surko, G. F. Gribakin, and S. J. Buckman, J. Phys. B **38**, R57 (2005).
[2] T. S. Pedersen, J. R. Danielson, C. Hugenschmidt, G. Marx, X. Sarasola, F. Schauer, L. Schweikhard, C. M. Surko, and E. Winkler, New J. Phys. **14**, 035010 (2012).
[3] N. Guessoum, P. Jean, and W. Gillard, Appl. Surf. Sci. **252**, 3352 (2006).
[4] C. Hugenschmidt, Surf. Sci. Rep. **71**, 547 (2016).
[5] D. W. Gidley, D. Z. Chi, W. D. Wang, and R. S. Vallery, Annu. Rev. Mater. Sci. **36**, 49 (2006).
[6] P. J. Schultz and K. G. Lynn, Rev. Mod. Phys. **60**, 701 (1988).
[7] *Principles and Practice of Positron Emission Tomography*, edited by R. L. Wahl (Lippincott, Williams and Wilkins, Philadelphia, PA, 2002).
[8] G. F. Gribakin, J. A. Young, and C. M. Surko, Rev. Mod. Phys. **82**, 2557 (2010).
[9] J. A. Young and C. M. Surko, Phys. Rev. A **77**, 052704 (2008).
[10] J. R. Danielson, A. C. L. Jones, M. R. Natisin, and C. M. Surko, Phys. Rev. A **88**, 062702 (2013).
[11] G. F. Gribakin, J. F. Stanton, J. R. Danielson, M. R. Natisin, and C. M. Surko, Phys. Rev. A **96**, 062709 (2017).
[12] G. F. Gribakin and C. M. R. Lee, Eur. Phys. J. D **51**, 51 (2009).
[13] A. C. L. Jones, J. R. Danielson, M. R. Natisin, C. M. Surko, and G. F. Gribakin, Phys. Rev. Lett. **108**, 093201 (2012).
[14] N. Guessoum, P. Jean, and W. Gillard, Mon. Not. R. Astron. Soc. **402**, 1171 (2010).
[15] K. Iwata, R. G. Greaves, and C. M. Surko, Can. J. Phys. **74**, 407 (1996).
[16] S. J. Gilbert, L. D. Barnes, J. P. Sullivan, and C. M. Surko, Phys. Rev. Lett. **88**, 043201 (2002).
[17] M. R. Natisin, J. R. Danielson, and C. M. Surko, Appl. Phys. Lett. **108**, 024102 (2016).
[18] R. G. Greaves and C. M. Surko, Can. J. Phys. **74**, 445 (1996).
[19] S. Ghosh, J. R. Danielson, and C. M. Surko, J. Phys. B **53**, 085701 (2020).
[20] M. R. Natisin, J. R. Danielson, and C. M. Surko, Phys. Plasmas **22**, 033501 (2015).
[21] D. M. Bishop and L. M. Cheung, J. Phys. Chem. Ref. Data **11**, 119 (1982).
[22] P. W. Pakes, T. C. Rounds, and H. L. Strauss, J. Phys. Chem. **85**, 2476 (1981).
[23] J. H. Schachtschneider and R. G. Snyder, Spectrochim. Acta **19**, 117 (1963).
[24] M. R. Natisin, J. R. Danielson, G. F. Gribakin, A. R. Swann, and C. M. Surko, Phys. Rev. Lett. **119**, 113402 (2017).
[25] G. F. Gribakin and C. M. R. Lee, Phys. Rev. Lett. **97**, 193201 (2006).
[26] A. C. L. Jones, J. R. Danielson, M. R. Natisin, and C. M. Surko, Phys. Rev. Lett. **110**, 223201 (2013).
[27] W. E. Wallace, director, Infrared spectra in *NIST Chemistry WebBook*, edited by P. J. Linstrom and W. G. Mallard (National Institute of Standards and Technology, Gaithersburg, 2020), https://doi.org/10.18434/T4D303.